Proc. Natl. Acad. Sci. USA
Vol. 96, pp. 9397–9402, August 1999
Neurobiology

Disrupted cortical map and absence of cortical barrels in growth-associated protein (GAP)-43 knockout mice

DONNA L. MAIER*, SHYAMALA MANI†, STACY L. DONOVAN*, DAN SOPPET‡§, LINO TESSAROLLO‡, JAMES S. MCCASLAND*, AND KARINA F. MEIRI†¶

Departments of *Anatomy and Cell Biology, and †Pharmacology, State University of New York Health Science Center, Syracuse, NY 13210; ‡National Cancer Institute/Frederick Cancer Research and Development Center, Building 539 Room 245, P.O. Box B, Fort Detrick, MD 21702-1201; and §Human Genome Sciences, 9410 Key West Avenue, Rockville, MD 20850

Edited by Richard L. Sidman, Harvard Medical School, Southborough, MA, and approved June 14, 1999 (received for review April 14, 1999)

ABSTRACT **There is strong evidence that growth-associated protein (GAP-43), a protein found only in the nervous system, regulates the response of neurons to axonal guidance signals. However, its role in complex spatial patterning in cerebral cortex has not been explored. We show that mice lacking GAP-43 expression (−/−) fail to establish the ordered whisker representation (barrel array) normally found in layer IV of rodent primary somatosensory cortex. Thalamocortical afferents to −/− cortex form irregular patches in layer IV within a poorly defined cortical field, which varies between hemispheres, rather than the stereotypic, whisker-specific, segregated map seen in normal animals. Furthermore, many thalamocortical afferents project abnormally to widely separated cortical targets. Taken together, our findings indicate a loss of identifiable whisker territories in the GAP-43 −/− mouse cortex. Here, we present a disrupted somatotopic map phenotype in cortex, in clear contrast to the blurring of boundaries within an ordered whisker map in other barrelless mutants. Our results indicate that GAP-43 expression is critical for the normal establishment of ordered topography in barrel cortex.**

The nervous-system-specific phosphoprotein GAP-43 plays an important role in regulating the response of growing axons to extracellular signals (1). Overexpressing GAP-43 causes ectopic sprouting *in vivo* (2), whereas GAP-43 knockout mice show defective retinal ganglion cell guidance (3, 4). However, the consequences of failure to express GAP-43 on cortical organization have not been investigated.

Somatotopic mapping of sensory surfaces is a fundamental principle of vertebrate brain organization. The one-to-one correspondence of large whiskers on the rodent face with cellular aggregates in the somatosensory cortex "barrels" has served as a powerful model of this principle (5). Visible whisker representations appear sequentially in the brainstem (barrelettes), thalamus (barreloids), and cortex during development (6, 7). The barrel field provides a sensory map that is readily manipulated and easily compared between individuals.

The cortical barrel field represents at least two levels of organization: topographic (somatotopic) and territorial. First, thalamocortical afferents (TCAs) from all whiskers form an ordered (topographic) representation in deep cortical layers (8). Next, TCAs from any particular whisker cluster in layer IV, thereby segregating from other afferents to form whisker-specific territories. Both processes are completed by postnatal day 7 (P7). Barrelless phenotypes have been described in which normal somatotopy was preserved, but barrels were not visible because TCA segregation or clustering was incomplete (9–12). Here, we present a mutant with disrupted (disordered) cortical somatotopy.

In normal rats, GAP-43 is expressed in a barrel-like pattern during P3–P7, when TCAs segregate. After barrel formation is complete, expression is down-regulated (and is simultaneously up-regulated in the septa between individual barrels; ref. 13). The expression pattern suggests GAP-43 involvement in the initial ordering of TCA axons, their subsequent segregation, or both. Using a GAP-43 knockout mouse that we created, we establish that, in the absence of GAP-43 expression, TCAs fail to extend to their appropriate targets in layer IV of cortex and that, as a consequence, they fail to establish an ordered whisker representation in layer IV of cortex.

MATERIALS AND METHODS

Targeting Vector and Generation of GAP-43 Mutant Mice. The targeting vector consisted of a 9.0-kilobase (kb) A129/sv genomic fragment, in which 476 bp of the GAP-43 gene (from intron 1 and nucleotides 133–171 from the cDNA) was replaced with the pGKneobpA cassette. The pGKTK cassette was the negative selection marker. Electroporation and selection used the CJ7 embryonic stem (ES) cell line. Genomic DNA from 313 G418/FIAU-resistant ES cell clones was screened by Southern analysis with 5′ and 3′ probes external to the targeting vector sequence. Multiplex PCR was used for genotyping the offspring of GAP-43 heterozygote crosses. The PCR mixture contained the primers shown in Fig. 1*a*: p1 (5′-GGCTCATAAGGCTGCAACCAAAAT-3′), p2 (5′-CCATCTCCCTCCTTCTTCTCCACA-3′), p3 (5′-CCGGCCGCTTGGGTGGAGAG-3′), and p4 (5′-TCGGCAGGAGCAAGGTGAGATGAC-3′). A 165-bp product was amplified from the wild-type allele between p1 and p2. A 299-bp product was generated from the mutant allele between p3 and p4. Heterozygotes amplified both fragments. p3 and p2 did not amplify under the conditions used. Care of all animals was in accordance with institutional guidelines.

General Histological Procedures. The perfusion procedure has been described (14). Frozen sections were cut tangential to the barrels or coronal at 40–50 μm, and thalamus sections were cut in horizontal, coronal, or horizontal oblique planes at 40–60 μm.

Histochemistry and Immunohistochemistry. All littermate sets of sections were incubated together. Sections from neonatal or adult mouse hemispheres were stained for Nissl or cytochrome oxidase (CO) histochemistry as described (15). For immunohistochemical studies, sections from hemispheres were reacted with one of two antibodies. The first recognized

The publication costs of this article were defrayed in part by page charge payment. This article must therefore be hereby marked "*advertisement*" in accordance with 18 U.S.C. §1734 solely to indicate this fact.

PNAS is available online at www.pnas.org.

This paper was submitted directly (Track II) to the *Proceedings* office.
Abbreviations: TCA, thalamocortical afferent; P*n*, postnatal day *n*; ES, embryonic stem; kb, kilobase; CO, cytochrome oxidase; FB, Fast Blue; DTR, dextran Texas-Red; VB, ventrobasal.
¶To whom reprint requests should be addressed. E-mail: meirik@hscsyr.edu.

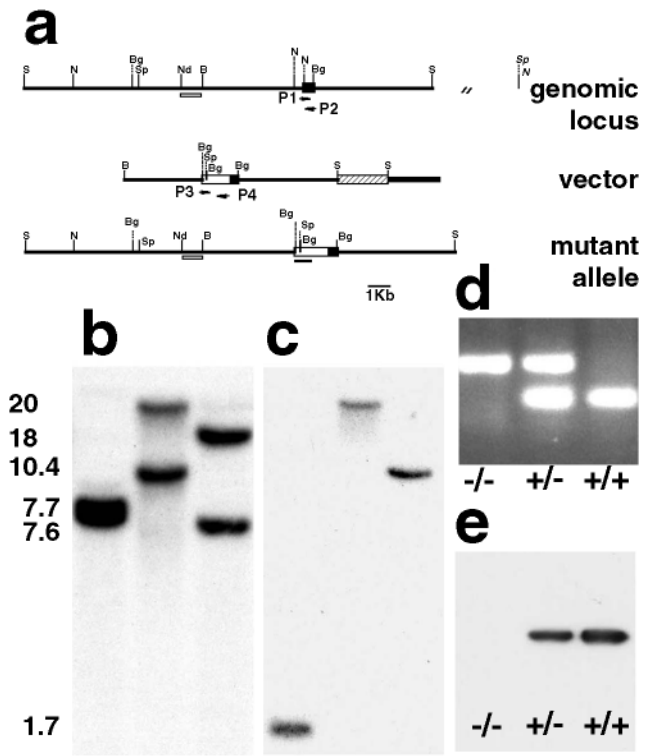

FIG. 1. (*a*) Structure of the GAP-43 locus (*Top*), the targeting vector (*Middle*), and the mutant allele (*Bottom*). The bacterial *neo*^{r} selection cassette pPGKneobpA (white box) was inserted into *Nhe*–*Nhe* sites at exon 2 (black box), the 1.6-kb fragment replacing 476 bp of the native gene. The 5′ external probe used for Southern analysis is shown by a white bar, and the neo probe is shown with a black bar. Arrows indicate the PCR primers used for genotyping progeny of heterozygote matings by PCR. The restriction enzymes used were B, *Bam*HI; Bg, *Bgl*I; E, *Eco*RI; N, *Nhe*I; Nd, *Nde*; S, *Sal*I; and Sp, *Spe*I. (*b* and *c*) Southern analysis of DNA from one heterozygote ES cell clone. (*b*) DNA was digested with *Bgl*I, *Nhe*I, and *Spe*I and then hybridized to the 5′ external probe. Bands from the wild-type allele are at 8.5 kb, 10.4 kb, and 18 kb, respectively, whereas the mutant allele has bands at 7.7 kb, 20 kb, and 7.6 kb. (*c*) The blot was reprobed with the 380-bp *neo* probe. The mutant allele gives rise to bands at 1.72 kb, 20 kb, and 10.4 kb, respectively. (*d*) PCR assay showing the three possible genotypes; homozygote (−/−), heterozygote (+/−), and wild type (+/+). (E) Western blot of P1 brain homogenates (lane 1, +/+; lane 2, +/−; and lane 3, −/−) probed with the anti-GAP-43 mAb 7B10 (50 μg of total protein per lane).

the serotonin transporter (5HT-T; Incstar, Stillwater, MN). The second was a rat monoclonal tenascin antibody (Sigma). Specific immunoreactivity was detected with biotinylated secondary antibodies and ABC reagent (Vector Laboratories) and visualized with diaminobenzidine.

Double Retrograde Tracer Experiments. Stereotaxic measurements determined tracer placement within the whisker-barrel field of adult (P82–P89) mice. Fast Blue (FB, Sigma) and dextran Texas-Red (DTR; molecular weight = 10,000; Molecular Probes) were infused into layer IV at separate locations 0.7–1.0 mm apart. After 3 days, the animals were perfused, and the brain was cryosectioned at 50 μm. Sections were examined by using UV and rhodamine filters. DTR and FB images were contrast-enhanced and superimposed by using layer blending to show the location of both tracers simultaneously.

RESULTS

Generation of GAP-43 Knockout Mice. Genomic DNA from 313 G418/FIAU-resistant ES cell clones was screened by Southern blot analysis (Fig. 1 *a*–*c*). Recombinant clones were obtained at a frequency of 1/156. GAP-43 recombinant ES clones injected into C57BL/6 blastocysts generated chimeras that transmitted the mutated allele to progeny when mated to C57BL/6 or A129/sv females. Similar Southern blotting and multiplex PCR (Fig. 1*d*) was used for genotyping. Heterozygous animals were viable and fertile. Breeding GAP-43 +/− mice gave rise to homozygous mutant mice at a 25% frequency. Homozygous (−/−) progeny failed to express GAP-43 (Fig. 1*e*). About 50% of them died within 2 days (P0–P2). Most of the remainder died between P14 and P21. A small percentage (<5%) survived weaning. Neonatal (P7) and adult (P30–P90) mice were used in these experiments. Two strains were examined: (*i*) the A129/sv strain in which the knockout was generated and (*ii*) the progeny of a seventh-generation backcross into C57BL/6. The phenotype was similar in both strains.

Absence of an Ordered Whisker Map in GAP-43 −/− Knockout Mice. The serotonin transporter (5HT-T) is a transient marker of thalamic neurons (15–17) and provides clear evidence that mapping of TCAs is disrupted in −/− animals. We used 5HT-T immunohistochemistry to define the developing barrel pattern in layer IV of normal somatosensory cortex (Fig. 2 *a* and *d*). In contrast, 5HT-T labeling of GAP-43 in −/− cortex consisted of irregularly shaped blotches in a presumptive barrel field whose edges were uneven and not clearly demarcated (Fig. 2 *b* and *c*). The marked variations in 5HT-T labeling between hemispheres showed that, although TCAs do cluster in layer IV of −/− cortex (Fig. 2 *e* and *f*), these clusters bear no consistent relationship to the stereotyped whisker pattern or thalamic barreloid array. These results are direct evidence that an ordered whisker map does not form in the absence of GAP-43.

Consistent with these results, the barrel pattern was not evident in −/− cortex with standard histological stains. Nissl staining identified cytoarchitectural contours of barrels in wild-type +/+ mice at P7 (Fig. 2*g*). In contrast, barrels could not be detected in −/− cortex (Fig. 2*h*). Similarly, we found no evidence of regular patterning in −/− cortex with tenascin immunoreactivity (Fig. 2, compare *j* −/− with *i* +/−), indicating that the septa delineating individual barrels were also absent in the knockout mice (18). Finally, CO histochemistry of barrel cortex [and of ventrobasal (VB) thalamus—see following section] showed reduced intensity and no discernable barrels in layer IV of the −/− animals (Fig. 2 *l* and *n*), whereas they were evident in both wild types +/+ (Fig. 2*k*) and heterozygotes +/− (Fig. 2*m*). The barrel array had not arisen in −/− mice even by P90, as seen by either CO histochemistry (Fig. 2*n*) or Nissl staining (not shown). Thus, formation of barrels is prevented permanently, not merely delayed, in the GAP-43 −/− mice.

Normal Whisker Representations in Trigeminal Brainstem Nuclei and Barreloid-Like Patches in the VB Nucleus. A previous study that used another GAP-43 −/− mouse reported grossly normal organization of nuclei, tracts, and cell layers by P20 (19). Transient disruptions in axonal outgrowth were described, but innervation of peripheral targets by the trigeminal nerve were normal (19). This study did not examine the corresponding central pathways. In our GAP-43 −/− mice, CO histochemistry showed whisker representations (barrelettes) in the trigeminal brainstem nuclei resembling those in wild-type animals (Fig. 3 *a*–*d*). In the VB thalamus of −/− mice, 5HT-T immunoreactivity showed clear evidence of axonal segregation into barreloid-like patches (Fig. 3, compare *i* and *j* with *k* and *l*), although the pattern was somewhat compromised relative to the normal animals. However, CO histochemistry marked a more reduced area in the VB thalamus and showed no clear evidence of barreloid patterning (Fig. 3, compare *e* and *f* with *g* and *h*). Thus it seems that, although the −/− phenotype is largely confined to the cortical map, as has been observed with other mutations that affect the

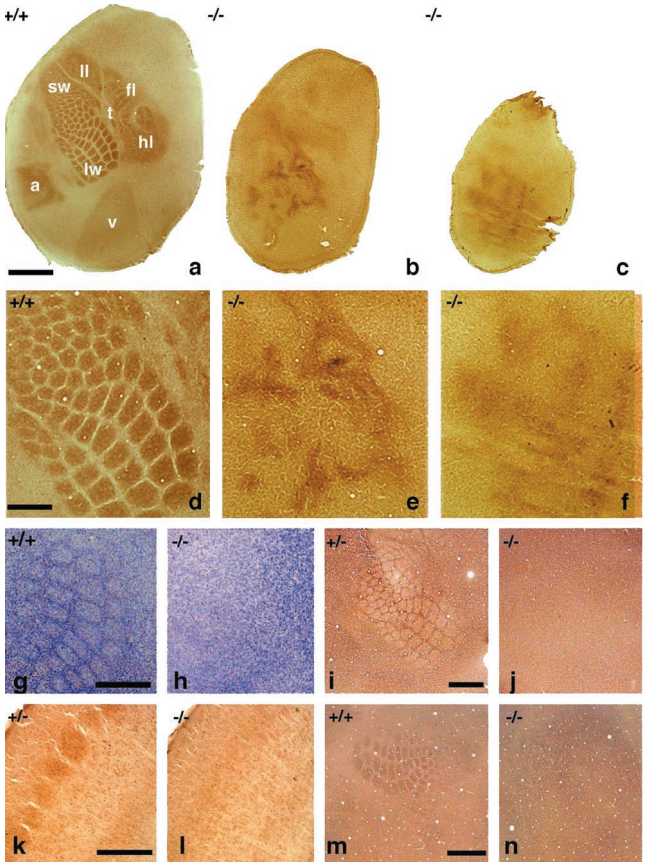

FIG. 2. (*a–f*) Tangential cortex from mice labeled with 5HT-T. (*a* +/+) A complete body map in layer IV (a, auditory cortex; v, visual cortex; hl, hindlimb; fl, forelimb; ll, lower lip; t, trunk; lw, large whiskers; sw, small whiskers), indicating somatotopy and segregation of TCAs. (*b* and *c* −/−) In contrast, tangential cortices show irregularly shaped blotches. The outer edges of the presumptive barrel field are uneven and not clearly demarcated. (Bar = 500 μm.) (*d* +/+; *e* and *f* −/−) At higher magnification, the blotches in −/− cortex do not resemble the normal whisker array seen in +/+ cortex. (Bar = 167 μm.) +/+, $n = 4$; +/−, $n = 4$, not shown; −/−, $n = 7$. (*g–j*) Nissl stain and tenascin immunoreactivity also clearly show the absence of normal cytoarchitectural contours and septa between individual barrels in GAP-43 −/− cortex. (*g* +/+ and *h* −/−) Nissl stain of tangential section through layer IV of left barrel cortex. (Bar = 200 μm.) +/+, $n = 5$; +/−, $n = 3$, not shown; −/−, $n = 2$. (*i* +/− and *j* −/−) P7 tenascin immunohistochemistry through a similar area. (Bar = 200 μm.) +/+, $n = 4$, not shown; +/−, $n = 4$; −/−, $n = 6$. (*k–n*) CO histochemistry shows reduced metabolic activity in the barrel area in GAP-43 −/− cortex. (*k* +/− and *l* −/−) CO histochemistry of coronal section of left barrel cortex, showing barrels in layer IV of +/− only (diagonal band from lower left to upper right of panel. Abnormally light histochemistry for CO in layer IV suggests low activation of the thalamocortical pathway. (Bar = 200 μm.) +/+, $n = 1$, not shown; +/−, $n = 7$; −/−, $n = 2$. (*m* +/+ and *n* −/−) CO histochemistry of tangential sections from P60 mice showing that barrels do not form later in development in −/− cortex. (Bar = 500 μm.) +/+, $n = 2$; +/−, $n = 3$, not shown; −/−, $n = 2$.

barrels (10–12), nevertheless abnormalities in metabolic activity can be detected in the thalamic region that projects to barrel cortex.

Abnormal Thalamocortical Pathfinding in −/− Cortex. Nonoverlapping injections of two retrograde tracers into barrel cortex (Fig. 4 *a* and *c*) showed that −/− thalamic neurons project to abnormally widespread cortical targets. In +/+ thalamus, retrogradely labeled cells were strictly segregated (Fig. 4 *b* and *Insert*), consistent with the cortical injections (Fig. 4*a*). In contrast, in −/− thalamus, labeled cells were dispersed with marked overlap between labels (Fig. 4 *d* and *Insert*). These

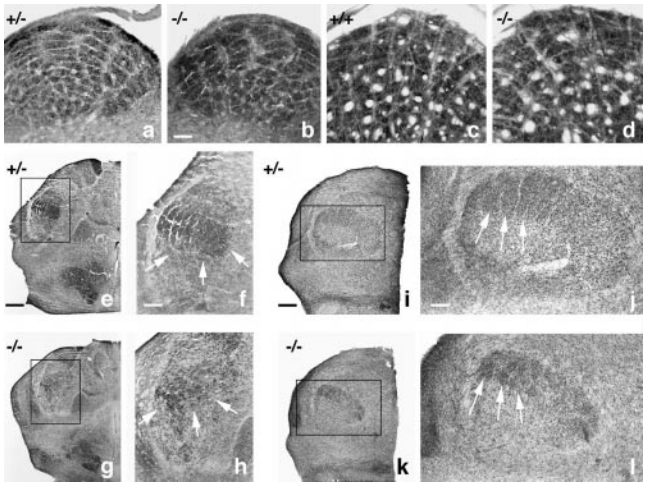

FIG. 3. (*a* +/− and *b* −/−) CO histochemistry of P7 trigeminal subnucleus interpolaris shows the brainstem whisker representation. (*c* +/+ and *d* −/−) CO histochemistry at P60 shows that the brainstem whisker representation persists in −/− mice. +/+, $n = 2$; +/−, $n = 2$, not shown; −/−, $n = 2$. (Bar = 100 μm.) (*e* and *f* +/−; *g* and *h* −/−) Horizontal section through left VB complex at P7 labeled by CO histochemistry of whisker representation (barreloids) in +/− mice (+/+ not shown). Higher magnification (*f* and *h*) of −/− mice shows that the boundaries of the VB thalamus are difficult to discern because of a much smaller area of intense CO labeling (arrows), suggesting that thalamic circuitry is relatively inactive. (*e* and *g*, Bar = 250 μm; *f* and *h*, Bar = 100 μm.) +/+, $n = 2$, not shown; +/−, $n = 3$; −/−, $n = 2$. (*i–l*) Horizontal oblique sections through the VB thalamus of P7 mice immunostained for 5HT-T show segregated barreloids in +/− and −/− thalamus. Higher magnification (*j* and *l*) shows that barreloid segregation in the −/− mouse (arrows) resembles +/+ (not shown) and +/−. (Bars = 100 μm.) +/+, $n = 2$; +/−, $n = 3$; −/−, $n = 2$.

data indicate that at least some −/− TCAs fail to order and segregate appropriately. However, some crude preservation of topography is suggested by the similar orientation of patches of labeled cells in −/− thalamus with respect to the cortical injections (Fig. 4, compare *a* and *c* with *b* and *d*).

Misrouted TCAs Show Imprecise Targeting in Cortex in the Absence of GAP-43. In the +/+ VB nucleus of the thalamus, DTR-labeled neurons were normally distributed and limited to a cluster roughly 300 μm deep (Fig. 5*a*). In contrast, DTR-labeled cells in −/− VB thalamus were uniformly distributed throughout the entire dorsoventral 600 μm examined (Fig. 5*a*). In +/+ VB thalamus only 0.03 ± 0.04% (mean ± SEM; $n = 2$) of labeled cell bodies in the volume occupied by the DTR-labeled cohort were blue. In contrast, in −/− VB thalamus, 63 ± 19% (mean ± SEM; $n = 3$) of labeled cells in the DTR-labeled zone were blue. The difference is statistically significant ($P < 0.01$, Student's *t* test), indicating that misrouting from the barreloid representations in the VB thalamus to layer IV of the cortex has occurred.

Abnormal TCA pathfinding in −/− cortex is also indicated by the aberrant laminar distribution of TCA terminals. The band of dense 5HT-T staining of TCAs in layer IV of +/+ cortex was much thinner in −/− mice (Fig. 4*g*). Normal arborization of TCAs in layer VI was also nearly absent (Fig. 4*h*), reflecting the abnormally light CO histochemistry in layers IV and VI, the laminae that normally receive dense thalamic projections (see Fig. 2*h*).

The abnormal laminar distribution of TCAs in −/− cortex is related in part to inappropriate branching. Fig. 4*h* (asterisk) shows the apparent branching of one 5HT-T-labeled TCA within deep layers of −/− cortex. Larger-than-barrel branching resulting in double labeling with both tracers occurred in 9.8 ± 0.03% (mean ± SEM; $n = 3$) of labeled TCA neuronal cell bodies in −/− VB thalamus. In contrast, only 0.25 ± 0.3%

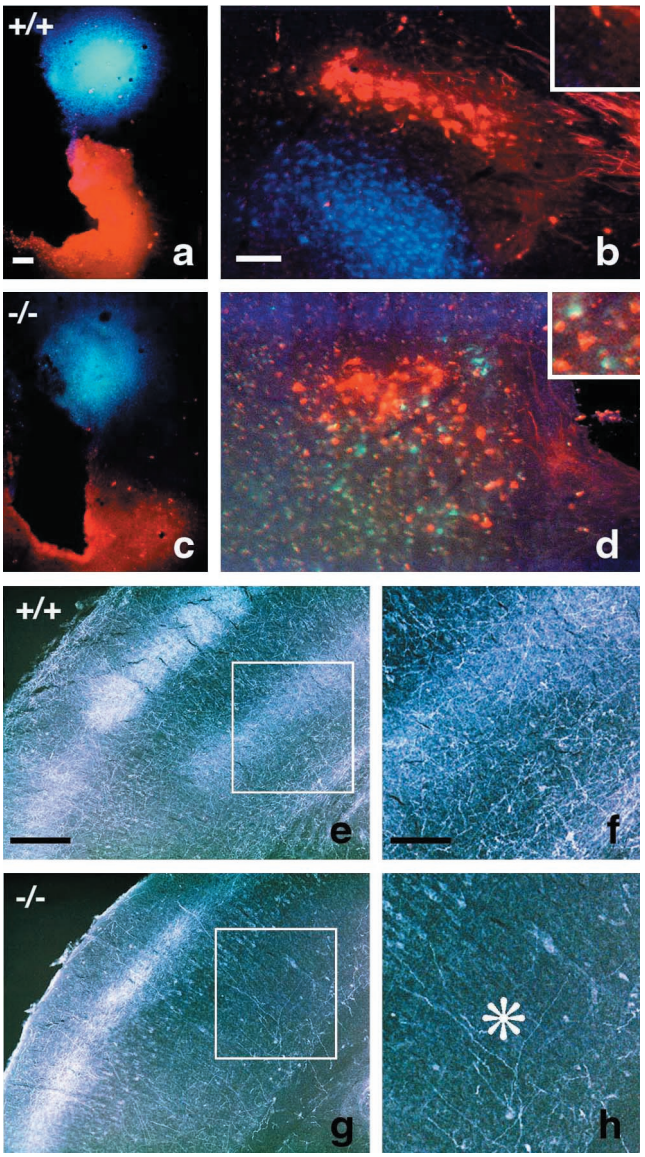

FIG. 4. (*a* +/+ and *c* −/−) Spatially distinct injections of two retrograde tracers (anterior, FB; posterior, DTR) into adult barrel cortex showed different patterns of labeling in VB thalamus. (*b* +/+) Zones of FB- and DTR-labeled cells were spatially discrete. (*d* −/−) Although crude topography of the two labels was maintained, zones of labeled cells overlapped with some double labeling (*Insert*). (*a* and *c*, Bars = 250 μm; *b* and *d*, Bars = 100 μm.) +/+, $n = 2$; +/−, $n = 4$, not shown; −/−, $n = 2$. (*e* +/+) Coronal sections at P7 labeled with 5HT-T with image inversion to identify segregated TCAs in layer IV and arborization in layer VI of cortex. (*f*) Higher magnification of box in *e*. (*g* −/−) Layer IV is thinner and not segregated into barrels. (*h*) Higher magnification of box in *g* shows that whisker-specific arborizations in layer VI are absent. The asterisk indicates branching of a TCA axon in cortex. (*e* and *g*, Bar = 200 μm; *f* and *h*, Bar = 100 μm.)

(mean ± SEM; $n = 2$) of cells were double labeled in the +/+ VB thalamus. The difference was statistically significant ($P < 0.01$, Student's *t* test). Together, the results show that both misrouting and inappropriate branching of TCAs occurs in the −/− mice.

DISCUSSION

These results indicate a disrupted (nonsomatotopic) cortical map phenotype. They also show that, in the absence of GAP-43, normally patterned thalamocortical connections fail to form. Previous reports have shown that barrel formation

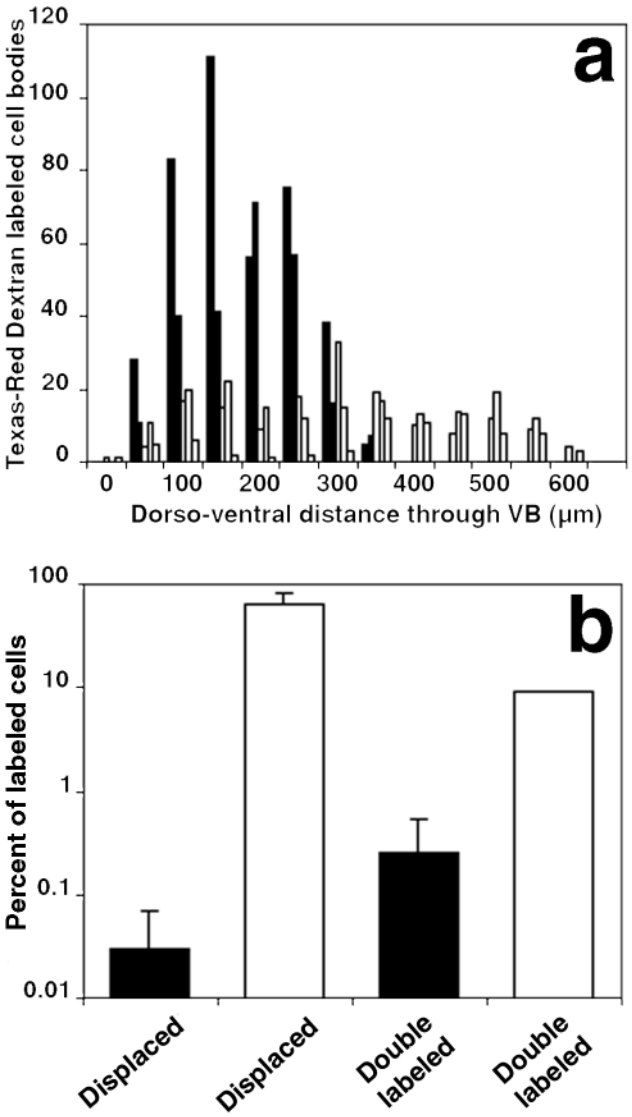

FIG. 5. (*a*) Distribution of DTR-labeled cell bodies in VB thalamus from counts of 15 50-μm serial sections. DTR-labeled cell bodies were normally distributed and discretely located in the VB thalamus (black bars; +/+; mean ± SEM = 319 ± 54; $n = 2$). Significantly fewer DTR-labeled cell bodies were dispersed throughout the sections (open bars; −/−; mean ± SEM = 158 ± 25; $n = 3$). ($P < 0.05$, Student's *t* test.) (*b*) Displacement and double labeling of labeled TCAs in the VB thalamus. (First black bar; +/+) Only 0.03 ± 0.04% (mean ± SEM; $n = 2$) of total labeled cells within the volume occupied by the DTR cohort were blue, confirming that the two labels remained desegregated. (First open bar; −/−) In contrast, 63 ± 19% (mean ± SEM; $n = 3$) of total labeled cells were blue, indicating displacement/misrouting of TCAs to cortex. ($P < 0.01$, Student's *t* test.) (Second black bar; +/+) Only 0.25 ± 0.3% (mean ± SEM; $n = 3$) of cell bodies incorporated both labels. (Second open bar; −/−) 9.8 ± 1.41% (mean ± SEM; $n = 3$) were double labeled, indicating inappropriate larger-than-barrel branching in TCAs ($P < 0.025$, Student's *t* test.)

(segregation) is prevented by a spontaneous mutation (9) disrupting the gene for adenylyl cyclase type I (10), by excessive serotonin production (11) and by reduced *N*-methyl-D-aspartate receptor synthesis (12). However, in each of these cases, topological order in the pattern of TCA arborization was preserved. In contrast, our phenotype shows a complete failure to establish an ordered cortical barrel map.

How can we be certain that the whisker map is disrupted? In the normal barrel field, cortical territories are competitively parceled into a regular array that fits mathematical principles minimizing nearest-neighbor distances (Dirichlet domains; ref.

20). These principles apply even when barrel fields are abnormal because of supernumerary (ectopically transplanted) whiskers or lesions to portions of the whisker pad. The irregular clustering of presumptive TCA terminals in −/− cortex violates this principle of parcellation; the mechanism that normally produces the regular somatotopic array must therefore be disabled. Even in the presence of an invariant facial whisker array and clearly recognizable thalamic barreloids, different −/− hemispheres show different patterns of TCA clustering (Fig. 2 *e* and *f*). Therefore, any mapping of whiskers in −/− cortex, even to misshapen whisker territories, is not consistent. The essence of the normal cortical map is the predictable relationship between periphery and cortex. The absence of this predictability in GAP-43 −/− cortex implies that there is no whisker "map" worthy of the name.

Our data suggest that the principal mechanism that causes the cortical map to be disrupted is aberrant thalamocortical pathfinding. Both 5HT-T immunohistochemistry and double retrograde labeling indicate an absence of arborization in layer VI, aberrant patterning in layer IV, and displacement of TCAs, suggesting pathfinding errors by thalamic axons. Normally, TCAs extend radially to layer IV from the subplate and segregate to form individual barrels (refs. 21 and 22; also see review in ref. 23). This radial growth pattern suggests that they first form a crude but topologically correct map in the cortical subplate (refs. 8 and 24; see also refs. 25 and 26). DiI-labeling (1,1′-dioctadecyl-3,3,3′,3′-tetramethylindocarbocyanine perchlorate-labeling) also shows axons apparently in good order in the internal capsule and the subplate (data not shown). Hence, we suspect that the disruption occurs after the initial formation of a crude subplate map. In fact, the evidence suggests a focal interruption in this transmission between the thalamus and cortex. In this regard, three of the four other mutant phenotypes showed no disruption of brainstem representations, and only ours had thalamic abnormalities (evident in the lack of CO patterning in VB thalamus). As a group, these results indicate that the concept of barrel development based solely on serial instruction from brainstem to thalamus to cortex must be reexamined. We suggest that serial instruction is necessary but not sufficient for the formation of cortical barrels.

The possibility that the map fails in part because of abnormal activity-mediated synaptic sorting cannot be ruled out. Low CO reactivity in layers IV and VI of −/− cortex as well as VB thalamus suggests that the irregular clustering of TCAs occurs in a relatively inactive synaptic environment (which may be caused by relatively sparse thalamic projections to these layers). It seems unlikely that the degree of long-range TCA misrouting implied by our data could be prevented merely by increased synaptic activity. However, TCAs in −/− cortex do form irregular clusters, a process that may well be driven by activity-dependent mechanisms (27, 28). If a deficit in TCA outgrowth is responsible for the failure to form barrels, it must be far more severe than the defect seen at the optic chiasm in the previous studies of GAP-43 −/− mice (3, 19), owing to the fact that this deficit in axonal navigation is transient and that our barrelless phenotype is permanent. Our phenotype is also unlikely to be solely a consequence of malnutrition, because malnourished animals form barrel maps of reduced size and with a delayed time course but with normal barrel segregation and topology (29).

A defect in thalamocortical pathfinding is consistent with localization of GAP-43 to axonal and presynaptic compartments and with its role in the growth cone to transduce extracellular guidance cues (1). In this regard, we have shown recently that central nervous system neurons from our GAP-43 −/− mice are unable to respond to neural cell adhesion molecule, L1, and *N*-cadherin signals that normally induce neurite outgrowth (30). The molecular nature of any such signals in the cortex—and, importantly, whether they are positive or negative—is under investigation. The apparent failure of many TCAs to terminate and arborize normally in layer IV might reflect a partial failure of TCAs to recognize hypothesized cortical stop signals (25).

In summary, we think there are three main reasons that the phenotype is largely cortical. First, the effect is likely to be cumulative, with errors in one station of the trigeminal pathway contributing to larger errors in the next. The reduction in both CO reactivity and 2-deoxyglucose labeling in thalamus and cortex suggests that activity-mediated effects may contribute to these cumulative errors. Second, single-axon labeling with the 5HT-T antibody indicates multiple axon branching in deep cortical layers; these branching errors are never observed in normal mice and may indicate a failure of specific TCA interactions with cells in either the subplate or other infragranular layers. Finally, previous studies showing that integrin-mediated responses are unaffected in the GAP-43 −/− mouse (19, 30) lead us to speculate that contact-mediated signaling may be more important in TCA pathfinding than in projections to subcortical stations in the pathway. This speculation may also account for the apparently normal trigeminal nerve projections (19).

GAP-43 has been shown to play multifunctional roles within different parts of the neuron at all stages of neuronal development (31). The present results show that its absence also has profound consequences on the establishment of both topographic organization and appropriate afferent segregation in cortex.

We thank Jan Blair, Ginny Graczyk, Susan Reid, Stacy Scicchitano, Yiping Shen, and Qi Zhang for expert technical assistance, Mary Blue for advice and helpful comments, and Jerry Miller for use of his confocal microscope. This work was supported by the National Cancer Institute (D.S. and L.T.), by National Institutes of Health Grants NS31829 (to J.S.M.) and NS33118 (to K.F.M.), and by National Science Foundation Grant 9724102 (to J.S.M.).

1. Benowitz, L. & Routtenberg, A. (1997) *Trends Neurosci.* **20,** 84–91.
2. Aigner, L., Arber, S., Kapfhammer, J. P., Laux, T., Schneider, C., Botteri, F., Brenner, H. R. & Caroni, P. (1995) *Cell* **83,** 269–278.
3. Kruger, K., Tam, A. S., Lu, C. & Sretavan, D. W. (1998) *J. Neurosci.* **18,** 5692–5705.
4. Zhu, Q. & Julien, J.-P. (1999) *Exp. Neurol.* **155,** 228–242.
5. Woolsey, T. A. & Van der Loos, H. (1970) *Brain Res.* **17,** 205–242.
6. Woolsey, T. A., Anderson, J. R., Wann, J. R. & Stanfield, B. B. (1979) *J. Comp. Neurol.* **184,** 363–380.
7. Durham, D. & Woolsey, T. A. (1984) *J. Comp. Neurol.* **223,** 424–447.
8. Agmon, A., Yang, L. T., Jones, E. G. & O'Dowd, D. K. (1995) *J. Neurosci.* **15,** 549–561.
9. Welker, E., Armstrong-James, M., Bronchti, G., Ourednik, W., Gheorghita-Baechler, F., Dubois, R., Guernsey, D. L., Van der Loos, H. & Neumann, P. E. (1996) *Science* **271,** 1864–1867.
10. Abdel-Majid, R. M., Leong, W. L., Schalkwyk, L. C., Smallman, D. S., Wong, S. T., Storm, D. R., Fine, A., Dobson, M. J., Guernsey, D. L. & Neumann, P. E. (1998) *Nat. Genet.* **19,** 289–291.
11. Cases, O., Vitalis, T., Seif, I., De Maeyer, E., Sotelo, C. & Gaspar, P. (1996) *Neuron* **16,** 297–307.
12. Iwasato, T., Erzurumlu, R. S., Huerta, P. T., Chen, D. F., Sasaoka, T., Ulupinar, E. & Tonegawa, S. (1997) *Neuron* **19,** 1201–1210.
13. Erzurumlu, R. S., Jhaveri, S. & Benowitz, L. I. (1990) *J. Comp. Neurol.* **292,** 443–456.
14. McCasland, J. S. (1996) *J. Neurosci. Methods* **68,** 113–123.
15. Bruning, G. & Liangos, O. (1997) *Acta Histochem.* **99**, 117–121.
16. Lebrand, C., Cases, O., Adelbrecht, C., Doye, A., Alvarez, C., El Mestikawy, S., Seif, I. & Gaspar, P. (1996) *Neuron* **17,** 823–835.
17. Bennet-Clark, C., Chiaia, N. & Rhoades, R. (1996) *Brain Res.* **733,** 301–306.
18. Steindler, D. A., Cooper, N. G., Faissner, A. & Schachner, M. (1989) *Dev. Biol.* **131,** 243–260.

19. Strittmatter, S. M., Fankhauser, C., Huang, P. L., Mashimo, H. & Fishman, M. C. (1995) *Cell* **80,** 445–452.
20. Senft, S. L. & Woolsey, T. A. (1991) *Cereb. Cortex* **1,** 348–363.
21. Jhaveri, S., Erzurumlu, R. S. & Crossin, K. (1991) *Proc. Natl. Acad. Sci. USA* **88,** 4489–4493.
22. Jhaveri, S., Erzurumlu, R. S., Laywell, E. D., Steindler, D. A., Albers, K. M. & Davis, B. M. (1996) *J. Comp. Neurol.* **374,** 41–51.
23. Rice, F. L. (1995) in *Cerebral Cortex: The Barrel Cortex of Rodents*, eds. Jones, E. G. & Diamond, I. T. (Plenum, New York), Vol. 11, pp. 1–75.
24. Agmon, A., Yang, L. T., O'Dowd, D. K. & Jones, E. G. (1993) *J. Neurosci.* **13,** 5365–5382.
25. Molnar, Z. & Blakemore, C. (1995) *Trends Neurosci.* **18,** 389–397.
26. Killackey, H. P., Rhoades, R. W. & Bennett-Clarke, C. A. (1995) *Trends Neurosci.* **18**, 402–407.
27. Crair, M. C. & Malenka, R. C. (1995) *Nature (London)* **375,** 325–328.
28. Isaac, J. T., Crair, M. C., Nicoll, R. A. & Malenka, R. C. (1997) *Neuron* **18,** 269–280.
29. Vongdokmai, R. (1980) *J. Comp. Neurol.* **191,** 283–294.
30. Meiri, K., Saffell, J., Walsh, F. & Doherty, P. (1998) *J. Neurosci.* **18,** 10429–10536.
31. Oestreicher, A. B., De Graan, P. N., Gispen, W. H., Verhaagen, J. & Schrama, L. H. (1997) *Prog. Neurobiol.* **53,** 627–686.